2024 IEEE 63rd Conference on Decision and Control (CDC)
December 16-19, 2024. MiCo, Milan, Italy

Modeling the development of drug resistance during chemotherapy treatment

Marcello Pompa, Dániel András Drexler, Simona Panunzi, Balázs Gombos,
András Füredi, Gergely Szakács, Levente Kovács, and Andrea De Gaetano

Abstract— **The development of drug resistance is a major obstacle in cancer treatment, leading to frequent tumor recurrence. Upon being first diagnosed, many tumors tend to respond well to chemotherapy, only to later display resistance to previously effective drugs. Understanding the mechanisms behind this emergent drug resistance is crucial for designing more effective treatment protocols. In this study, we present a novel mathematical model that investigates the competition between heterogeneous tumor cell populations with varying metabolic strategies and drug resistance profiles. Rather than hypothesizing metabolic plasticity (cells switching metabolic pathways), our model hypothesizes the coexistence of two (or more) cell populations, of which one has greater growth potential and greater drug sensitivity than the other. Considering this metabolic heterogeneity, together with potentially flexible, environment-induced genetic variations, would help us better characterize variable tumor response to treatment. The model parameters are here estimated using data from mice tumors treated with pegylated liposomal doxorubicin. Simulations using the model reveal that an initial period of drug sensitivity, during which the tumor shrinks, can mask the expansion of a small subpopulation of metabolically less efficient but drug-resistant cells. Over time, the resistant subpopulation outcompetes the originally expanding, metabolically more efficient subpopulation, leading to the observed resurgence of the tumor in a drug-resistant form.**

I. INTRODUCTION

Cyber-medical systems comprise many engineering and IT solutions applied in medicine. Physiological control is an emerging approach that can enhance therapy for many diseases, e.g., cancer [1]–[3], artificial pancreas [4]–[9], or control of anesthesia [10]–[12]. These approaches are based on mathematical models, which are then personalized to the patient through identification techniques and, finally, therapy is generated by control engineering or other mathematical optimization methods.

Chemotherapy optimization methods rely on mathematical models describing the effect of the drug on tumor dynamics. There are some results of therapy optimization validated with mice experiments [1], [2], using a simple mathematical model [13], [14]. A notable difference of this model from other models in the literature is that it contains dead tumor dynamics, which is important in the applications since, generally, the measured tumor contains both living and dead tumor cells. Most models in the literature lack these features. For a review of the tumor models, see, e.g., [15], [16]. Most models in the literature describe living tumor cell dynamics and pharmacokinetics, some incorporate immune cell and healthy cell dynamics (the models describing immunotherapy), and the dynamics of the vascular support of the tumor (the models describing antiangiogenic therapy).

Development of resistance during therapy is a critical issue that often leads to inefficient therapy and the death of the patient [17]. Modeling resistance acquired during the therapy may help us understand the nature of the process through simulation and develop treatment strategies that can reduce the chance of resistance. Greene et al. published a model that can describe drug resistance [18], where there is a population of sensitive and resistant cells that compete with each other. The sensitive cells proliferate faster than the resistant cells, but as the sensitive cells die due to the treatment, the resistant cells gain ground for proliferation, and the tumor becomes resistant to the drug [19].

We introduce a model in Section III, which describes the tumor as being composed of three parts: the sensitive, the resistant, and the dead tumor cells. Similar to the model created by Greene et al. [18], we model the competition of the cell populations and the mutation that may turn sensitive cells into resistant cells. Significant differences in our approach reside in the use of an exponential growth form for the two cell subpopulations and in the inclusion of dead cells for the total volume calculation (as dead cells are not eliminated instantly from the organism, but turn into scar tissue). Moreover, in this work, a procedure for the model parameter estimation was carried out by adapting the mathematical model to experimental data. The results of the

Marcello Pompa, Simona Panunzi, and Andrea de Gaetano are with the Institute of Systems Analysis and Informatics "A. Ruberti" (IASI) - National Research Council of Italy, Rome, Italy. Andrea de Gaetano is also with the Research and Innovation Center of Obuda University, Obuda University, Budapest, Hungary, and the Institute for Biomedical Research and Innovation (IRIB) - National Research Council of Italy, Palermo, Italy. (emails: marcello.pompa@biomatematica.it, simona.panunzi@biomatematica.it, andrea.degaetano@biomatematica.it)

Dániel András Drexler and Levente Kovács are with the Physiological Controls Research Center, Research and Innovation Center of Obuda University, Obuda University, Budapest, Hungary. (emails: drexler.daniel@uni-obuda.hu, kovacs@uni-obuda.hu)

Balázs Gombos and András Füredi are with the Drug Resistance Research Group, Research Center for Natural Sciences, Budapest, Hungary. Balázs Gombos is also with the Semmelweis University, Molecular Medicine PhD School, Budapest, Hungary. András Füredi is also with the Institute of Technical Physics and Materials Science, HUN-REN Centre of Energy Research, Budapest, Hungary. (emails: gombos.balazs@ttk.hu, furedi.andras@ttk.hu)

Gergely Szakács is with the Center for Cancer Research, Medical University of Vienna, Vienna, Austria. He is also with the Drug Resistance Research Group, Research Center for Natural Sciences, Budapest, Hungary. (email: gergely.szakacs@meduniwien.ac.at)

979-8-3503-1632-2/24/$31.00 ©2024 IEEE

fitting procedure are reported in Section IV. We define the experimental setting and the parameter estimation approach in Section II, and end the paper with conclusions in Section V.

II. METHODS

In Section IV, we fit the model introduced in the next section to measurements from mouse experiments. We discuss the experimental setting in Subsection II-A, and the fitting process in Subsection II-B.

A. Experimental settings

We use data from experiments that were carried out to test our previously published therapy optimization methods [1], [2] on a clinically relevant, genetically engineered mouse model of breast cancer. The Brca1, a DNA repair gene, and p53, a regulator of cell cycle and genome stability, were knocked out in breast epithelial cells. Thus, the resulting mammary tumors highly resemble the Brca1-linked, triple-negative, hereditary breast cancer in humans: the molecular, immunohistochemical, morphological, and genetic characteristics are almost indistinguishable from their human counterparts [20]. These tumors in the mice respond to chemotherapy very similarly; initial treatment with doxorubicin significantly reduces tumor size and induces remission. However, long-term therapy often fails due to the emergence of drug resistance [21].

We use the data of six mice from the experiment. These mice received a 4 mg·kg^{-1} dose of Pegylated Liposomal Doxorubicin (PLD) the first time the tumor volume reached 200 mm^3. After tumor remission, when the tumor started to grow and reached 200 mm^3 again, we applied our strategies, model predictive control [2] and PDPK control [1]. The tumor size was measured with a digital caliper, and a formula was used to approximate the tumor volume [22]. This tumor is composed of living and dead tumor cells; this gave rise to the need to model dead tumor cell dynamics.

The doses were provided in mg·kg^{-1}; the injected dose was calculated using the weight of the mouse. The available data for model fitting are the tumor volume approximations based on caliper measurements, tumor weight measurements, and the injected doses in mg· kg^{-1}.

B. Parameter estimation

The model was adapted to experimental data obtained from the experimental procedure described in the previous subsection. Data over time from six mice were used in an Ordinary Least-Squares estimation procedure [23] to obtain mouse-specific parameter estimates. Each mouse presented about 50 experimental time points, and the parameter vector consisted of 6 free parameters.

The Runge-Kutta 4 method was used for integrating the model equations with a fixed time step of $0.1day$. The model implementation and parameter estimation were performed using Julia V1.9.3.

The parameters of the model introduced in the next section are shown in Table II, which contains the free, determined, or fixed ("given") parameters. As the model could be over-parameterized, some parameters were kept fixed to specific values obtained with preliminary estimation procedures and with calibration. The choice of which parameters is most reasonable to leave free to vary was made by considering the smallest set of parameters able to represent the phenomenon under study, as well as able to differentiate between two characteristic behaviors: mice that respond to the therapy and mice that develop a resistance to the chemotherapy.

For example, the competition effect between the two cell populations has been evaluated by fixing λ_{12} and estimating only parameter λ_{21}. Parameter ρ_{VX}, which is used to calculate tumor volume from the number of tumor cells, was calculated by considering the diameter of a cell of about 6-8μm. The algorithm used for optimizing the objective function was the Nelder-Mead method [24].

TABLE I

THE STATES VARIABLES AND THE INPUT OF THE MODEL.

Variable	Units	Meaning
X_1	#	Number of tumor cells sensitive to therapy
X_2	#	Number of tumor cells resistant to therapy
Z	#	Number of dead cells
X	#	Total number of cells
V	mm^3	Tumor volume
U	mg	Drug level in the administration compartment
u	mg· kg^{-1}	Dose of the administered drug
Y	mg	Drug level in the absorption compartment

III. MATHEMATICAL MODEL

The model developed in this work is structured in two submodels, five differential and two algebraic equations. The variables are summarized in Table I, and the 18 parameters of the model are shown in Table II. The mathematical formulation includes the presence of two types of cells (sensitive and resistant to the therapy) [18], [19]. Moreover, the contribution of the scar tissue [25], mainly composed of dead cells, is also considered in the total tumor volume calculation.

The first submodel describes the pharmacokinetics of the drug and the drug administration as

$$\begin{aligned} \dot{U} &= -k_{YU}U + \sum_{i=1}^{N} \delta(t - t_i)u_i M_i \\ U(t_0) &= U_0 \end{aligned} \tag{1}$$

$$\begin{aligned} \dot{Y} &= k_{YU}U - k_{EY}Y \\ Y(t_0) &= Y_0 \end{aligned} \tag{2}$$

where U represents the kinetics of the administered drug, u_i is the i-th dose of drug, administered at time t_i, and N is the total number of drug administrations. M_i is the mass of the mouse at time t_i, and Y represents the bioavailable drug that produces the effect on the tumor cells.

The second submodel represents tumor growth, considering a sensitive and resistant tumor cell population, and dead

TABLE II

MODEL PARAMETERS. IN THE "VALUE" COLUMN A NUMBER IS REPORTED WHEN THE RELATIVE PARAMETER IS FIXED AT A CERTAIN VALUE (FROM CALIBRATION OR A PRELIMINARY ESTIMATION PROCEDURE); THE WORD "FREE" IS USED IN THE CASE THE PARAMETER IS LEFT FREE TO BE TUNED AND IS THEREFORE ESTIMATED; PARAMETERS DESIGNED AS "DETERMINED" ARE COMPUTED FROM THE INITIAL CONDITIONS; "GIVEN" PARAMETERS ARE PROVIDED FROM EXPERIMENTS.

Parameter	Units	Meaning	Value
k_{11}	day^{-1}	tumor cell proliferation rate	free
λ_{12}	#	parameter representing the sensitivity of the X_1 growth rate to X_2	0.0005
ρ_{21}	day^{-1}	rate of X_1 that converts to X_2 subpopulation	free
k_{22}	day^{-1}	X_2 tumor cell proliferation rate	free
λ_{21}	#	parameter representing the sensitivity of the X_2 growth rate to X_1	free
k_{Z1}	day^{-1}	X_1 elimination rate	0.06
k_{Z2}	day^{-1}	X_2 elimination rate	0.06
k_{EZ}	day^{-1}	Z elimination rate	0.2
η_{Z1Y}	mg$^{-1}\cdot$ day^{-1}	effect of the therapy on X_1	free
η_{Z2Y}	mg$^{-1}\cdot$ day^{-1}	effect of the therapy on X_2	free
ρ_{VX}	mm^3 per million of cells	volume conversion factor	0.2
X_{10}	#	X_1 at time $t = 0$	determined
X_{20}	#	X_2 at time $t = 0$	0
k_{EY}	day^{-1}	drug absorption rate	0.25
k_{YU}	day^{-1}	drug transport rate from compartment U to compartment Y	0.3
Z_0	#	Z at time $t = 0$	0
X_0	#	X at time $t = 0$	determined
V_0	mm^3	V at time $t = 0$	given

tumor cells. Thanks to their higher proliferation rate, the most responsive (i.e., the sensitive) tumor cells compete with the drug-resistant subpopulation until the latter outcompetes the original one, leading to therapy resistance and tumor increase. This can happen when the sensitive population decreases due to therapy, and its inhibiting effect on the resistant cell population growth decreases significantly.

The dynamics of the sensitive cell population is described by

$$\begin{aligned} \dot{X}_1 &= k_{11}X_1e^{-\lambda_{12}X_2} - \rho_{21}X_1 - k_{Z1}X_1 - \eta_{Z1Y}YX_1 \\ X_1(t_0) &= X_{10} \end{aligned} \tag{3}$$

with X_1 being the number of sensitive tumor cells. The first term in the differential equation defines the proliferation (with competition with the resistant cells X_2), the second term describes that sensitive cells can mutate and become resistive cells, and the third term defines necrosis. The last term describes the effect of the drug.

The dynamics of the resistive cell population is given by

$$\begin{aligned} \dot{X}_2 &= \rho_{21}X_1 + k_{22}e^{-\lambda_{21}X_1}X_2 - k_{Z2}X_2 - \eta_{Z2Y}YX_2 \\ X_2(t_0) &= X_{20} \end{aligned} \tag{4}$$

where X_2 is the number of resistant cells. The first term in the differential equation describes the mutation of the resistant cells, the second term describes the cell proliferation (with the competition with the sensitive cells), the third term describes the necrosis, and the last term describes the effect of the drug. Note that resistant does not mean total resistance against the drug; the resistant cell population is only less sensitive to the drug compared to the sensitive population, i.e., for the parameters η_{Z1} and η_{Z2} we have that $\eta_{Z1} > \eta_{Z2}$.

The dynamics of the dead tumor cells is described as

$$\begin{aligned} \dot{Z} &= k_{Z1}X_1 + \eta_{Z1Y}YX_1 + k_{Z2}X_2 + \eta_{Z2Y}YX_2 - k_{EZ}Z \\ Z(t_0) &= Z_0 \end{aligned} \tag{5}$$

where Z is the number of dead cells. The first term defines the necrosis of the sensitive cells, the second term describes the effect of the drug on the sensitive cells, the third term represents the necrosis of the resistant cells, and the fourth term describes the effect of the drug on the resistant cells. The last term describes the washout of the dead cells.

The total number of tumor cells and their initial value are given by

$$\begin{aligned} X &= X_1 + X_2 + Z, \\ X(t_0) &= X_0 = X_{10} + X_{20} + Z_0, \end{aligned} \tag{6}$$

while the total (i.e., the measured) tumor volume is

$$\begin{aligned} V &= \rho_{VX}X, \\ V(t_0) &= \rho_{VX}X_0. \end{aligned} \tag{7}$$

In the absence of therapy, it is assumed that the number of resistant population cells is equal to zero (at the beginning of the experiment, there is still no mutation process); the number of dead cells is set at zero; therefore the initial number of total cells is equal to the number of cells sensitive to the therapy. Thus, from (7) it follows that

$$X_{10} = X_0 = \frac{V_0}{\rho_{VX}}. \tag{8}$$

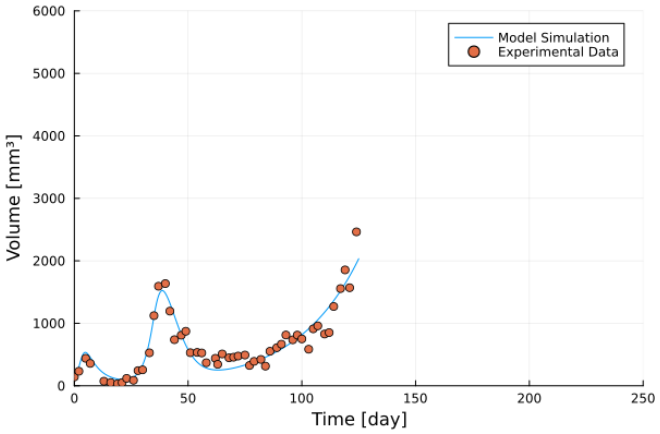

Fig. 1. Measurement and simulation results for the total tumor volume of mouse 1.

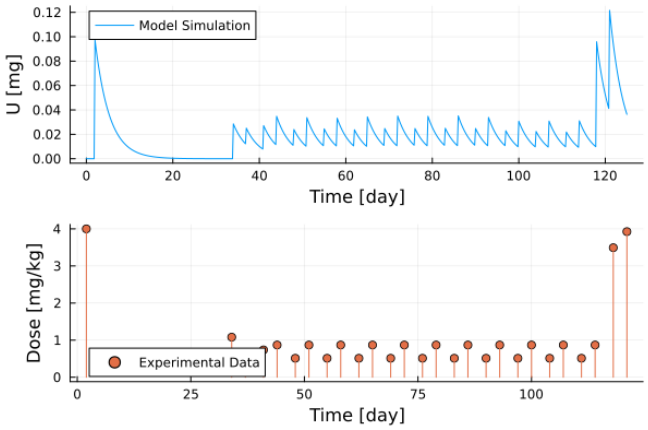

Fig. 2. Dosages and drug level over time for the mouse 1.

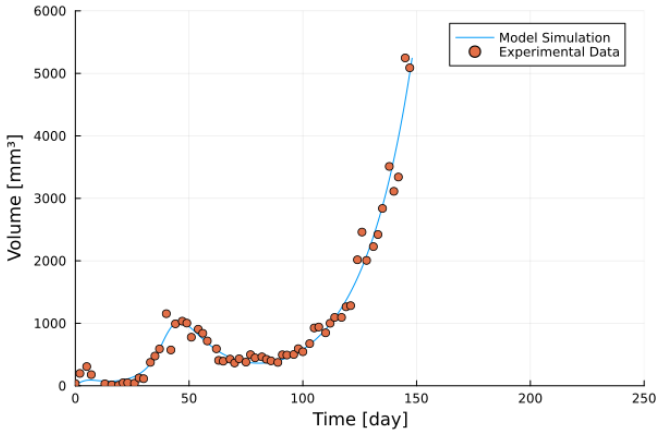

Fig. 3. Measurement and simulation results for the total tumor volume of mouse 2.

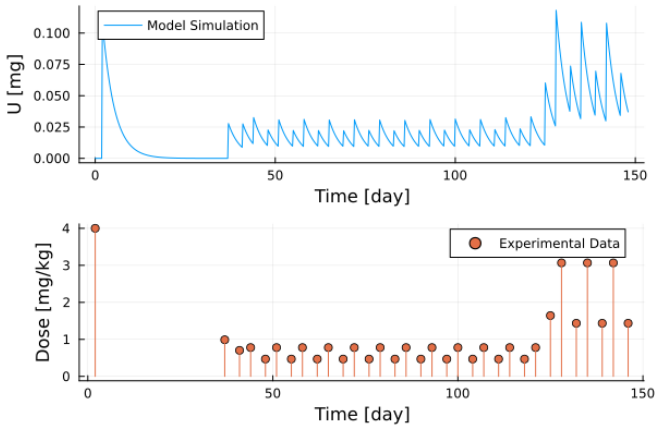

Fig. 4. Dosages and drug level over time for the mouse 2.

IV. RESULTS

The results of the model fit are presented in Figs. 1-12. Figures 1, 3, 5, 7, 9, and 11 show the tumor volume measurements denoted with red dots and the results carried out with the simulation of the fitted model for mice 1,2, ..., 6, respectively. The corresponding injected doses and the simulated drug levels in the administration compartment are shown in Figs. 2, 4, 6, 8, 10, and 12. The parameters resulting from the parameter estimation are shown in Tables III and IV.

The six mice in the experiments showed two different behaviors: tumors in mice 1,2 and 3 developed resistance during the treatment, and their tumor started to grow exponentially regardless of the injected drug. We will call this group of mice the "Resistant" group. Tumors in mice 4, 5, and 6 showed no resistance during the therapy; their tumors did not start to grow exponentially during treatment. We will call this group the "Not Resistant" group.

The different behaviors are reflected in the obtained parameters shown in Tables III and IV. Table III contains parameters for the "Resistant" group, and Table IV contains parameters for the "Not Resistant" group.

Although parameter η_{Z1}, representing the drug effect on the sensitive cells, is similar for both groups, we see a significant difference in the parameter η_{Z2} representing the effect of the drug on the resistant cell population. In the "Resistant" group, the value of η_{Z2} is smaller than in the "Not Resistant" group. The mean of parameter η_{Z2} in the "Not Resistant" group is 336% of the mean of the same parameter in the "Resistant" group. This reflects that the "Resistant" group is less sensitive to the drug than the "Not Resistant" group, which is in line with the hypotheses of the modeling.

The value of the parameter $k_{EZ} = 0.2\,[1/day]$, even if obtained from a calibration procedure, is perfectly comparable to the value of parameter $w = 0.214\,[1/day]$ (Dead tumor cell washout) in the work of L. Kovács et al. [2].

Regarding the tumor dynamics parameters, the growth rate of the sensitive cells k_{11} is similar in both groups, with a mean value in line with the parameter value $a = 0.226\,[1/day]$ (Tumor growth rate) from [2]. This is also true for the mutation rate ρ_{21}, which characterizes the rate of mutation of the sensitive cells into resistant cells. However, in the case of the "Resistant" group, the proliferation rate of the resistant cells (k_{22}) is larger (the mean is 248%

TABLE III

MODEL PARAMETER ESTIMATES OF THE "RESISTANT" GROUP (MICE 1,2, AND 3).

Parameters	Mouse 1	Mouse 2	Mouse 3	Mean	Standard Deviations
k_{11}	0,475583	0,273432	0,191653	0,31356	0,14615614
ρ_{21}	0,054943	0,029465	0,000106	0,02817	0,02744105
k_{22}	0,096442	0,106717	0,137548	0,11357	0,02139278
λ_{21}	0,044887	0,001539	0,007941	0,01812	0,02339861
η_{Z1Y}	22,92304	8,355523	10,54997	13,9428	7,85409636
η_{Z2Y}	6,91E-14	0,007749	0,046335	0,01803	0,02481878

TABLE IV

MODEL PARAMETER ESTIMATES OF THE "NOT RESISTANT" GROUP (MICE 4,5, AND 6).

Parameters	Mouse 4	Mouse 5	Mouse 6	Mean	Standard Deviations
k_{11}	0,499719	0,252323	0,472718	0,408254	0,135712754
ρ_{21}	0,056246	0,008369	0,02918	0,031265	0,024006644
k_{22}	0,047043	0,051064	0,038818	0,045642	0,00624229
λ_{21}	5,19E-08	3,69E-16	2,92E-12	1,73E-08	2,99599E-08
η_{Z1Y}	22,43253	9,369059	24,22907	18,67689	8,110711154
η_{Z2Y}	0,034729	0,113285	0,034136	0,060717	0,045526682

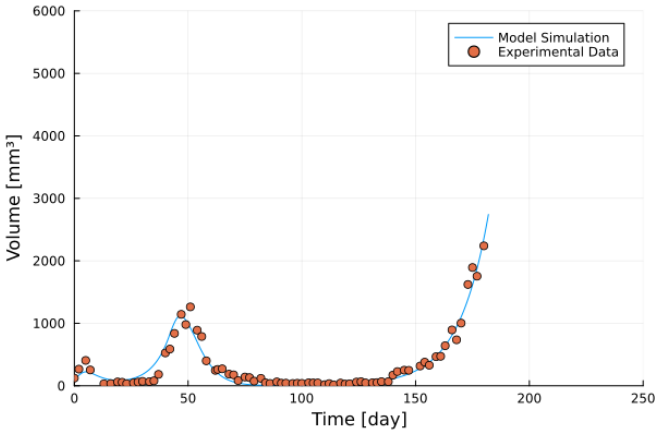

Fig. 5. Measurement and simulation results for the total tumor volume of mouse 3.

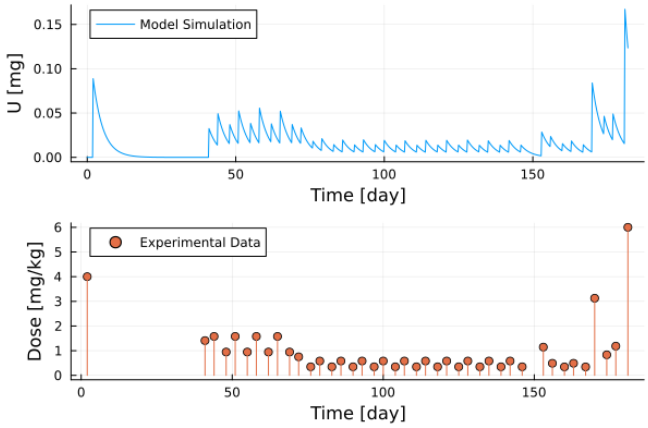

Fig. 6. Dosages and drug level over time for the mouse 3.

compared to the "Not Resistant" group). This implies that when the sensitive cell population becomes small enough to have a small inhibiting effect on the proliferation of the resistant cells, we can examine a steep growth in the resistant population.

There is a significant difference in the parameter λ_{21} characterizing the competition between the sensitive and resistant tumor cells. In the case of the "Not Resistant" group, this parameter is almost zero, showing that the sensitive cells have no significant effect on the growth of the resistant cells. This means that the treatment can eliminate the resistant cells; there is no need for the taming effect of the sensitive cells. It also gives rise to simplification of the model, i.e., we can neglect the resistant cell dynamics, getting back a model similar to the one used in our experiments [1], [2], [14].

However, in the case of the "Resistant" group, parameter λ_{21} is not zero. This means that initially, the sensitive tumor cells hold the resistant cells back from proliferating. When the size of the sensitive cell population decreases, this effect decreases as well, which leads to the increased proliferation of the resistant cells.

V. CONCLUSIONS

The model introduced in Section III aims to describe the development of drug resistance through modeling a sensitive and resistant cell population. The model also contains a second-order pharmacokinetic model of the drug and the dynamics of the dead tumor cells, making it suitable for modeling the dynamics of a tumor mass consisting of living and dead cells.

The parametric identification showed results that validated the hypotheses of the model, i.e., in the case of developed resistance, the effect of the drug on the resistant population is smaller, while the proliferation rate of the resistant cells is larger compared to the case when no resistance is developed during the treatment. An interesting result showed that in the cases when there was no resistance during the treatment, the effect of the sensitive cells on the resistant cell proliferation was negligible. This suggests that the model, if no resistance develops, can be simplified by removing the dynamics of the resistant cells.

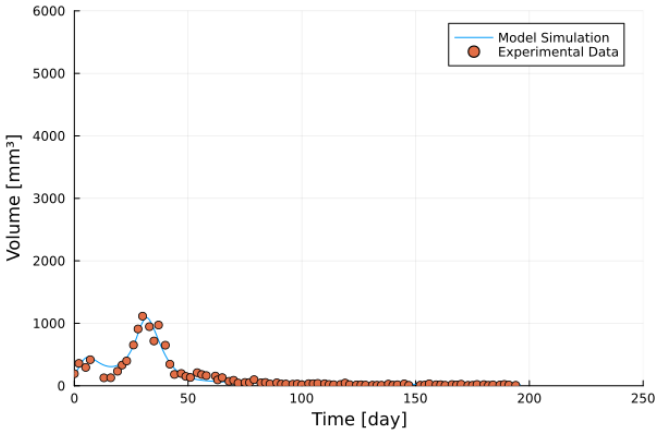

Fig. 7. Measurement and simulation results for the total tumor volume of mouse 4.

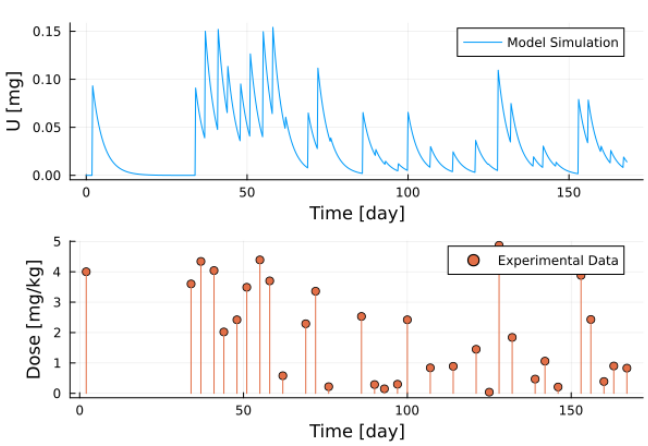

Fig. 8. Dosages and drug level over time for the mouse 4.

The results suggest that the model has the potential to be used in a future study, where a larger population of mice would increase the amount of experimental data and facilitate the validation process. It would be interesting to set up an experiment aimed at identifying the different types of tumor cells and establishing the ratio of resistant cells to sensitive cells under different therapy regimes. Moreover, the inclusion of the mice diet in the model, as well as the consideration of a saturation effect for the therapy due to a limited cell receptor availability, could be interesting improvements in a future study.

It has been hypothesized that the competition between drug-resistant and drug-sensitive cells can be exploited to prevent the development of resistance during treatment. By strategically eliminating sensitive cells with an optimized protocol, it is possible to hinder the expansion of emerging resistant cells. This approach aims to maintain a balance that suppresses the resistant population, ensuring that drug resistance does not render the therapy ineffective. The model proposed in this study can be used to design such therapies in the future.

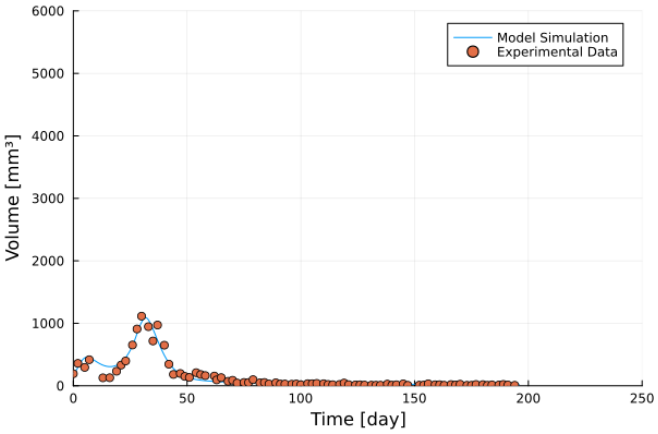

Fig. 9. Measurement and simulation results for the total tumor volume of mouse 5.

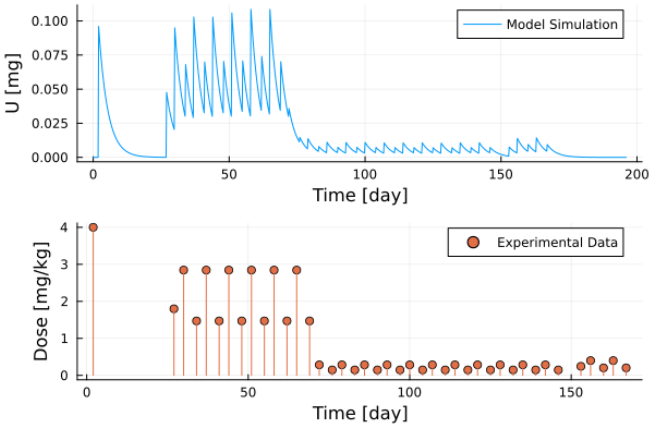

Fig. 10. Dosages and drug level over time for the mouse 5.

VI. ACKNOWLEDGMENTS

Project no. 2019-1.3.1-KK-2019-00007. has been implemented with the support provided from the National Research, Development and Innovation Fund of Hungary, financed under the 2019-1.3.1-KK funding scheme. This project has been supported by the Hungarian National Research, Development and Innovation Fund of Hungary, financed under the TKP2021-NKTA-36 funding scheme. The work of Dániel András Drexler was supported by the Starting Excellence Researcher Program of Obuda University, Budapest Hungary. The work of Prof. Andrea De Gaetano was supported by the Distinguished Professor Excellence Program of Obuda University, Budapest Hungary.

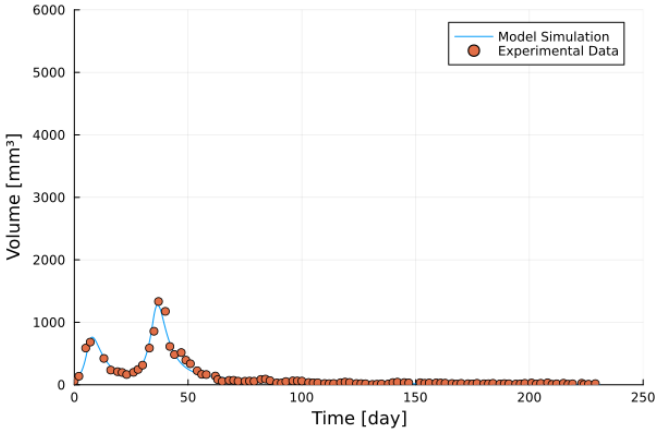

Fig. 11. Measurement and simulation results for the total tumor volume of mouse 6.

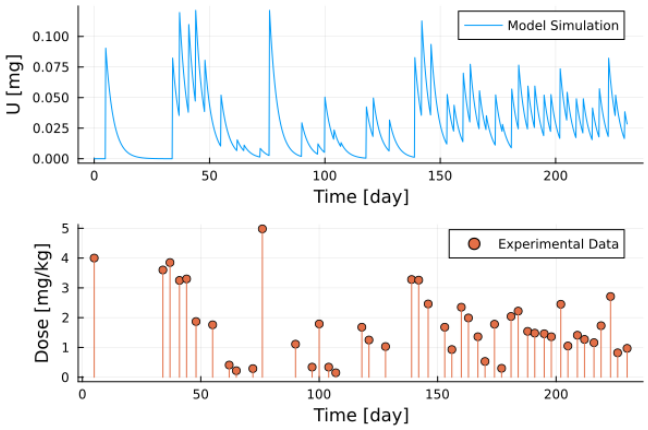

Fig. 12. Dosages and drug level over time for the mouse 6.

REFERENCES

[1] L. Kovács, T. Ferenci, B. Gombos, A. Füredi, I. Rudas, G. Szakács, and D. A. Drexler, "Positive impulsive control of tumor therapy—a cyber-medical approach," *IEEE Transactions on Systems, Man, and Cybernetics: Systems*, vol. 54, no. 1, pp. 597–608, 2024.

[2] L. Kovács, B. Czakó, M. Siket, T. Ferenci, A. Füredi, B. Gombos, G. Szakács, and D. A. Drexler, "Experimental closed-loop control of breast cancer in mice," *Complexity*, pp. 1–10, 2022.

[3] F. Cacace, V. Cusimano, A. Germani, P. Palumbo, and F. Papa, "Closed-loop control of tumor growth by means of anti-angiogenic administration," *Mathematical Biosciences & Engineering*, vol. 15, no. 4, pp. 827–839, 2018. [Online]. Available: https://doi.org/10.3934/mbe.2018037

[4] L. Kovács, "Linear parameter varying (LPV) based robust control of type-I diabetes driven for real patient data," *Knowledge-Based Systems*, vol. 122, pp. 199–213, 2017.

[5] R. Gondhalekar, E. Dassau, and F. J. Doyle, "Velocity-weighting & velocity-penalty MPC of an artificial pancreas: Improved safety & performance," *Automatica*, vol. 91, pp. 105 – 117, 2018.

[6] D. Shi, E. Dassau, and F. J. Doyle III, "Multivariate learning framework for long-term adaptation in the artificial pancreas," *Bioengineering & Translational Medicine*, vol. 0, no. 0, 2018.

[7] V. Moscardó, J. L. Díez, and J. Bondia, "Parallel control of an artificial pancreas with coordinated insulin, glucagon, and rescue carbohydrate control actions," *Journal of Diabetes Science and Technology*, vol. 13, no. 6, pp. 1026–1034, 2019.

[8] P. Szalay, D. A. Drexler, and L. Kovács, "Exploring robustness in blood glucose control with unannounced meal intake for type-1 diabetes patient," *Acta Polytechnica Hungarica*, vol. 20, no. 8, 2023.

[9] P. Colmegna, J. L. Díaz, J. Garcia-Tirado, and M. D. Breton, "Enabling anticipatory response in multi-stage MPC formulation for fully automated artificial pancreas system," in *2022 IEEE 61st Conference on Decision and Control (CDC)*, 2022, pp. 2566–2571.

[10] M. Alamir, M. Fiacchini, I. Queinnec, S. Tarbouriech, and M. Mazerolles, "Feedback law with probabilistic certification for propofol-based control of BIS during anesthesia," *International Journal of Robust and Nonlinear Control*, vol. 28, no. 18, pp. 6254–6266, 2018.

[11] C.-M. Ionescu, "A computationally efficient hill curve adaptation strategy during continuous monitoring of dose-effect relation in anaesthesia," *Nonlinear Dynamics*, vol. 92, no. 3, pp. 843–852, 2018.

[12] M. Ghita, D. Copot, I. R. Birs, C. I. Muresan, R. D. Keyser, M. Neckebroek, M. M. R. F. Struys, and C. M. Ionescu, "Uncertainty minimization and feasibility study for managing the complex and interacting anesthesia-hemodynamic system," in *2022 IEEE 61st Conference on Decision and Control (CDC)*, 2022, pp. 6064–6069.

[13] D. A. Drexler, J. Sápi, and L. Kovács, "Modeling of tumor growth incorporating the effects of necrosis and the effect of bevacizumab," *Complexity*, pp. 1–11, 2017.

[14] D. A. Drexler, T. Ferenci, A. Lovrics, and L. Kovács, "Tumor dynamics modeling based on formal reaction kinetics," *Acta Polytechnica Hungarica*, vol. 16, pp. 31–44, 2019.

[15] P. M. Altrock, L. L. Liu, and F. Michor, "The mathematics of cancer: integrating quantitative models," *Nature Reviews. Cancer*, vol. 15, no. 12, pp. 730–745, 2015.

[16] A. M. Jarrett, E. A. B. F. Lima, D. A. Hormuth, M. T. McKenna, X. Feng, D. A. Ekrut, A. C. M. Resende, A. Brock, and T. E. Yankeelov, "Mathematical models of tumor cell proliferation: A review of the literature," *Expert Review of Anticancer Therapy*, vol. 18, no. 12, pp. 1271–1286, 2018.

[17] A. Füredi, K. Szebényi, S. Tóth, M. Cserepes, L. Hámori, V. Nagy, E. Karai, P. Vajdovich, T. Imre, P. Szabó, D. Szüts, J. Tóvári, and G. Szakács, "Pegylated liposomal formulation of doxorubicin overcomes drug resistance in a genetically engineered mouse model of breast cancer," *Journal of Controlled Release*, vol. 261, pp. 287–296, 2017.

[18] J. M. Greene, J. L. Gevertz, and E. D. Sontag, "Mathematical approach to differentiate spontaneous and induced evolution to drug resistance during cancer treatment," *JCO Clinical Cancer Informatics*, vol. 3, pp. 1–20, 2019.

[19] W. Stein, J. Gulley, J. Schlom, R. Madan, W. Dahut, W. Figg, Y. Ning, P. Arlen, D. Price, S. Bates, and T. Fojo, "Tumor regression and growth rates determined in five intramural NCI prostate cancer trials: the growth rate constant as an indicator of therapeutic efficacy," *Clinical Cancer Resistance*, vol. 17, no. 4, pp. 907–914, 2011.

[20] X. Liu, H. Holstege, H. van der Gulden, M. Treur-Mulder, J. Zevenhoven, A. Velds, R. M. Kerkhoven, M. H. van Vliet, L. F. A. Wessels, J. L. Peterse, A. Berns, and J. Jonkers, "Somatic loss of BRCA1 and p53 in mice induces mammary tumors with features of human BRCA1-mutated basal-like breast cancer," *Proceedings of the National Academy of Sciences*, vol. 104, no. 29, pp. 12 111–12 116, 2007.

[21] S. Rottenberg, A. O. H. Nygren, M. Pajic, F. W. B. van Leeuwen, I. van der Heijden, K. van de Wetering, X. Liu, K. E. de Visser, K. G. Gilhuijs, O. van Tellingen, J. P. Schouten, J. Jonkers, and P. Borst, "Selective induction of chemotherapy resistance of mammary tumors in a conditional mouse model for hereditary breast cancer," *Proceedings of the National Academy of Sciences*, vol. 104, no. 29, pp. 12 117–12 122, 2007.

[22] J. Sápi, L. Kovács, D. A. Drexler, P. Kocsis, D. Gajári, and Z. Sápi, "Tumor volume estimation and quasi-continuous administration for most effective bevacizumab therapy," *PLoS ONE*, vol. 10, no. 11, pp. 1–20, 2015.

[23] A. L. Burton, "OLS (linear) regression," *The encyclopedia of research methods in criminology and Criminal Justice*, vol. 2, pp. 509–514, 2021.

[24] S. Singer and J. Nelder, "Nelder-Mead algorithm," *Scholarpedia*, vol. 4, no. 7, p. 2928, 2009.

[25] W. A. Weber and H. Wieder, "Monitoring chemotherapy and radiotherapy of solid tumors," *European Journal of Nuclear Medicine and Molecular Imaging*, vol. 33, no. 1, pp. 27–37, Jul 2006. [Online]. Available: https://doi.org/10.1007/s00259-006-0133-3